

# Decoherence and dephasing in strongly driven colliding Bose-Einstein condensates

N. Katz, R. Ozeri, E. Rowen, E. Gershnel and N. Davidson  
*Department of Physics of Complex Systems,  
 Weizmann Institute of Science, Rehovot 76100, Israel*

We report on a series of measurements of decoherence and wavepacket dephasing between two colliding, strongly coupled, identical Bose-Einstein condensates. We measure, in the strong excitation regime, a suppression of the mean-field shift, compared to the shift which is observed for a weak excitation. This suppression is explained by applying the Gross-Pitaevskii energy functional. By selectively counting only the non-decohered fraction in a time of flight image we observe oscillations for which both inhomogeneous and Doppler broadening are suppressed, in quantitative agreement with a full Gross-Pitaevskii equation simulation. If no post selection is used, the decoherence rate due to collisions can be extracted, and is in agreement with the local density average calculated rate.

The dephasing of a momentum excitation in a non-uniform Bose-Einstein condensate (BEC) is governed by several factors [1], [2]. Notably, the inhomogeneous broadening of the Bogoliubov energy shift and the Doppler broadening. We denote these processes as dephasing since they involve a reversible, although non-linear, evolution of the macroscopic wavefunction. In contrast, the decoherence of such an excitation due to collisions with the BEC, involves coupling to a quasi-continuum of initially unoccupied momentum states [3]. This process is driven by the fluctuating ground-state occupation of these modes, and is therefore inherently irreversible on timescales larger than the so called "memory time" of the system [4].

In previous works the inhomogeneous lineshape was

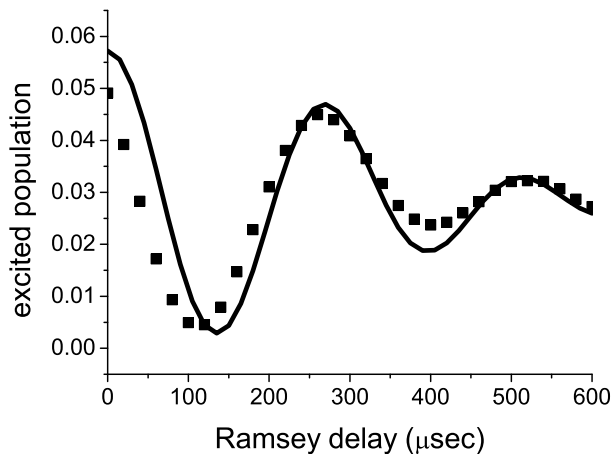


FIG. 1: Ramsey dephasing calculation. We simulate, by solving the cylindrically symmetric GPE [11], a Ramsey type experiment (solid boxes). We apply a detuned ( $\sim 3$  kHz) and weak  $40 \mu\text{sec}$  Bragg pulse, wait a variable Ramsey delay time, and then apply a second pulse which is in-phase with the first. A simplified local density averaging is also shown (solid line, described in the text), and is seen to capture the essence of the more complete simulation. Both curves decay at roughly the expected [1] inhomogeneous dephasing rate (3.0 kHz). [10]

seen to agree, for short Bragg coupling times, with both the experimental data [5], [6], and with simulations of the Gross-Pitaevskii equation (GPE) [7]. At longer timescales the inhomogeneous lineshape is resolved into radial modes [6]. Weak probe Bragg spectroscopy and interferometry were also used to characterize the coherence and spatial correlation function of condensates [8] and quasi-condensates [9]. In this letter we measure the dephasing and decoherence of strongly driven oscillations between two identical colliding BECs. By post selecting the non-decohered fraction we observe a strong suppression of both inhomogeneous and Doppler broadening mechanisms, which is in quantitative agreement with the results of a GPE simulation. The observed collisional decoherence rate is seen to agree with the expected local density approximation (LDA) average of the free particle collision rate.

The RMS width of the LDA inhomogeneous lineshape for high momentum excitations is given by  $\sqrt{8/147}\mu$ , where  $\mu$  is the chemical potential of the BEC [1]. The RMS Doppler broadening is given by,  $\sqrt{8/3}\hbar k/mR_z$  [1], where  $k$  is the wavenumber of the excitation,  $m$  is the mass of the BEC atom and  $R_z$  is the Thomas-Fermi radius of the condensate. For our experimental parameters the Doppler dephasing rate is predicted to be 0.6 kHz, which is clearly dominated by the expected 3.0 kHz inhomogeneous dephasing rate [10]. A GPE simulation [11] of the final excited population in a weak Bragg/Ramsey type experiment (an initial  $40 \mu\text{sec}$  weak coupling Bragg pulse, followed by a delay, and then a second pulse in phase with the first), with simulation parameters as described for our experimental system below, is shown in Fig. 1 (solid boxes). A simplified LDA of the Ramsey signal (solid line), taking only the density inhomogeneity into account, is seen to be in agreement with the full simulation. Here the weakly excited state, in the Bloch vector picture, precesses around the effective inhomogeneous local detuning, and this leads to decaying oscillations in the total final excited population. The calculated inhomogeneous dephasing rate of 3.0 kHz for our system agrees roughly with the Ramsey signal both in

the simulation and in LDA theory. We conclude that weak excitations, at short times, are well understood by LDA theory [8].

We now turn to the case of a strong excitation, i.e. where population of the zero-momentum condensate is completely (or nearly) depleted and transferred coherently to a travelling condensate in a Rabi-like oscillation. For sufficiently large  $k$ , the momentum of the excitation, we approximate such states by  $\psi(r, z) = a\phi_0(r, z) + be^{ikz}\phi_0(r, z)$  [12], where  $a$  and  $b$  are the amplitudes of the effective two level system and  $|a|^2 + |b|^2 = N$ , with  $N$  being the total number of atoms.  $\phi_0(r, z)$  is the ground-state wavefunction of the system with no excitations. The energy of such a state  $\psi$  can be evaluated by the Gross-Pitaevskii energy functional [13]  $E = \int dV \{ \frac{\hbar^2}{2m} |\nabla\psi(r, z)|^2 + V_0(r, z)|\psi(r, z)|^2 + \frac{g}{2} |\psi(r, z)|^4 \}$ , where  $V_0$  is the external potential and  $g$  is the mean-field coupling constant. By differentiating the energy by the excited state population  $|b|^2$ , and considering the result as a function of  $|b|^2$ , we find a population dependant excitation energy. For our experimental system we find a nearly linear decrease in excitation energy from the Bogoliubov prediction (weak excitation) at low  $|b|^2$ , via the free particle value at  $|b|^2 = N/2$  down to a symmetrically downshifted energy for  $|b|^2 \approx N$ , where the zero-momentum state is simply a weak excitation of the travelling condensate. The intuitive picture is that the energy per particle required to transfer the condensate from  $|b|^2 = 0$  to  $|b|^2 = N$  is simply the free particle energy, since the internal interaction energy is not changed by such a transformation. At sufficiently large Rabi frequencies, that achieve complete population inversion, the temporary mean field detuning averages to zero due to its symmetric nature, and the resonance shifts to the free particle value.

Our experimental apparatus is described in [14]. Briefly, a nearly pure ( $> 90\%$ ) BEC of  $1.6(\pm 0.5) \times 10^5$   $^{87}\text{Rb}$  atoms in the  $|F, m_f\rangle = |2, 2\rangle$  ground state, is formed in a QUIC type magnetic trap [15]. The trap is cylindrically symmetric, with radial ( $\hat{r}$ ) and axial ( $\hat{z}$ ) trapping frequencies of  $2\pi \times 226$  Hz and  $2\pi \times 26.5$  Hz, respectively. This corresponds to  $\mu/h = 2.48$  kHz.

We excite the condensate at a well defined wavenumber using two-photon Bragg transitions [16]. The two Bragg counter-propagating (along  $\hat{z}$ ) beams are locked to a Fabri-Perot cavity line, detuned 44 GHz below the  $5S_{1/2}, F = 2 \rightarrow 5P_{3/2}, F' = 3$  transition. At this detuning and at the intensities used here, there are no discernable losses from the condensate due to spontaneous emission. The frequency difference  $\delta\omega$  between the two lasers is controlled via two acousto-optical modulators. Bragg pulses of variable duration and intensity are applied to the condensate, controlling the excitation process.

Following the Bragg pulse, the magnetic trap is rapidly turned off, and after a 38 msec of time of flight expansion the atomic cloud is imaged by an on-resonance absorp-

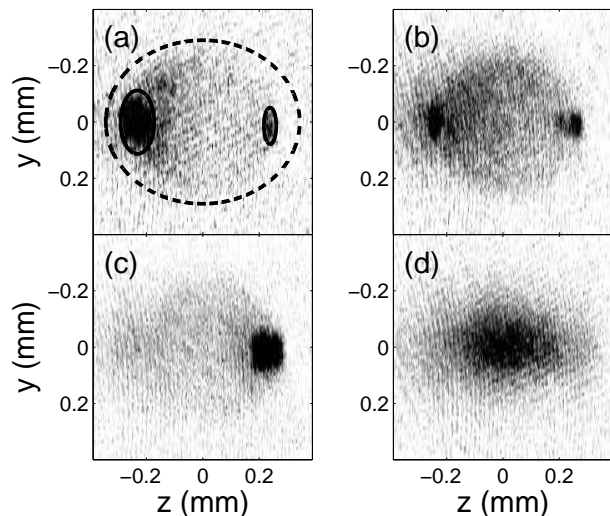


FIG. 2: Time of flight images of oscillating and colliding BECs. (a) A weak perturbation of the BEC (left, in solid line ellipse) to the excited population (right, in solid line ellipse). The dashed line marks the region of interest for measuring the average momentum  $P_{tot}$  (b) A  $\pi/2$  pulse, note the strong collisional sphere. (c) Almost a  $\pi$  pulse, note the weak collisional sphere, indicating collisions between the excitation and the zero momentum BEC. (d) After further oscillation ( $> 10\pi$  at 8.6 kHz), the BECs are completely decohered, and the Bragg coupling no longer effects the system.

tion beam, perpendicular to the  $\hat{z}$ -axis. Fig. 2 shows the resulting absorption images, for different excitation strengths and duration. Fig. 2a shows a perturbative excitation with the large cloud at the left corresponding to the BEC. A halo of scattered atoms is visible between the BEC and the cloud of unscattered outcoupled excitations to the right. In Fig. 2b we show a  $\pi/2$  pulse which generates a nearly symmetric excitation. The two condensates collide producing a strong collisional sphere. In Fig. 2c we show a nearly complete  $\pi$  pulse, with a weak zero momentum component remaining as an excitation of the travelling condensate. We note the weak thermal cloud surrounding the origin, which is largely unaffected by the Bragg pulse. When we increase the duration time of Rabi oscillations (Fig. 2d), the effective two level system is eventually depleted by collisions.

We measure the response of our system by integrating over the elliptical areas shown in Fig. 2a. The solid lines are gaussian fit areas to the uncollided atoms. The dashed line contains the entire region of interest, including the collisional products. We define the number of atoms observed in the excited region inclosed in the ellipse to the right as  $N_k$  and those corresponding to the initial BEC (left) as  $N_0$ .  $P_{tot}$  is the total momentum (in units of the momentum of a single excitation) along  $\hat{z}$  measured inside the dashed ellipse, and normalized by the overall number of observed atoms.

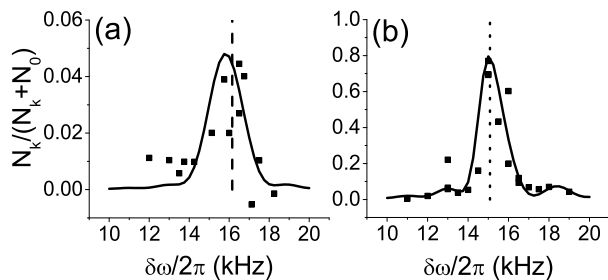


FIG. 3: Measured Bragg response (solid boxes) spectroscopy ( $N = 0.9 \times 10^5$ , and pulse duration of 0.5 msec for these measurements). Solid lines are GPE simulations (a) Weak excitation spectrum exhibiting the usual mean-field shifted Bogoliubov excitation resonance. The dashed line is at the theoretical LDA excitation energy (16.15 kHz). (b) Strong excitation spectrum, in which a clear suppression of the mean-field shift is observed. The dotted line is at the free particle excitation energy (15.08 kHz).

The suppression of the mean-field shift in strongly excited condensates is shown in Fig. 3b, where the resonance is clearly ( $14.9 \pm 0.2$  kHz from a gaussian fit) in agreement with the free particle value (15.08 kHz, indicated by the dotted line). This should be compared to the resonance ( $16.05 \pm 0.2$  kHz from a gaussian fit) observed in Fig. 3a for a weak excitation in agreement with the expected LDA value of 16.15 kHz (indicated by the dashed line). The solid lines are GPE simulations of the system, which also confirm the suppression of the mean-field shift.

This suppression of the mean-field shift should cause a similar decrease in the inhomogeneous broadening, leading to longer coherence times for strongly driven condensates. We explore this at various driving Rabi frequencies (but holding  $\delta\omega = 2\pi \times 15$  kHz constant). Fig. 4a and 4b show  $P_{tot}(t)$  at the driving frequencies of 1.2 kHz and 8.6 kHz, respectively. Fig. 4c and 4d show  $N_k/(N_0 + N_k)(t)$ , for the same driving frequencies.

The dashed lines in Fig. 4a and 4b are exponentially decaying oscillations, fitted to the experimental points. Here the decay is mainly due to collisions between the two condensates. The solid lines in Fig. 4c and 4d are GPE simulations with no fit parameters. We observe the remarkable result that by post-selecting the non-collided fraction we can recover the GPE dephasing behavior, despite the fact that the GPE totally disregards collisions between the excitations and the BEC and considers only the evolution of the macroscopic wavefunction.

The results of this analysis are summarized in Fig. 5. Here the solid boxes show the measured dephasing decay rate of  $N_k/(N_0 + N_k)(t)$ . An additional experimental point is measured at the Bragg driving frequency of 3.4 kHz. The solid line represents the theoretical dephasing rate obtained by numerically solving the GPE and then

fitting the time evolution to an oscillating exponential decay.

The empty boxes are the fitted decay rate of the oscillations in  $P_{tot}(t)$ . The dashed line is the result of the theoretical sum of the GPE dephasing rate calculated above (solid line), plus the free particle LDA collision rate (1.66 kHz) [17], with no fitting parameters.

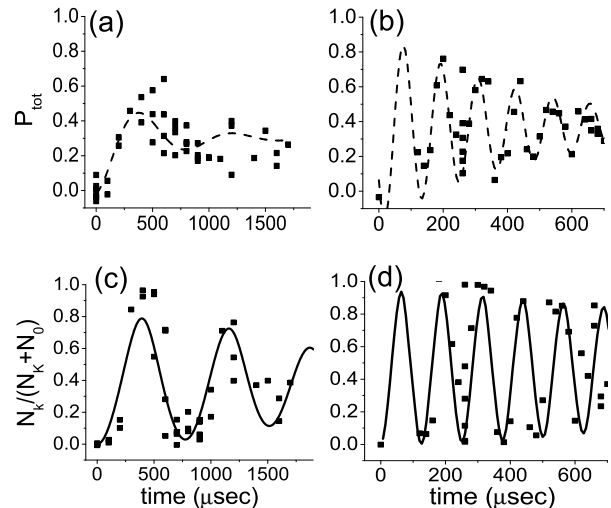


FIG. 4: Experimental oscillations between two coupled BECs (solid boxes) (a-b) average momentum  $P_{tot}$  at 1.2 (a) and 8.6 (b) kHz oscillations. The oscillations are damped due to collisions. The dashed lines in (a) and (b) are exponentially decaying oscillation fits to the points. (c-d) Post-selection of the uncollided fraction  $N_k/(N_0 + N_k)$  for the 1.2 (c) and 8.6 (d) kHz oscillations. The solid lines in (c) and (d) are GPE simulations with no fitting parameters.

There are several points of interest in this figure. Firstly, we note that the suppression of inhomogeneous effects is again confirmed both in simulation and in experiment. This can be observed by the minima of the simulation curve at 3 kHz driving frequency. The experimental data agrees with this trend. Where the observed decay rates of  $P_{tot}$  and  $N_k/(N_0 + N_k)$  are 2 and 10 times smaller, respectively, than the calculated inhomogeneous dephasing rate (as shown in Fig. 1).

Secondly, the GPE simulation dephasing rate ( $\sim 0.1$  kHz) near 3 kHz driving frequency is significantly slower than the Doppler dephasing rate (0.6 kHz). The experimental points agrees with this trend. This suppression can be understood by considering the system in the frame of reference of the travelling light potential [18]. In this reference frame the condensate is on the edge of the Brillion zone, and is repeatedly reflected by the potential. Due to the strong lattice potential, there is a broad region in momentum space for which the group velocity is zero. Consequently, the two wavepackets do not separate, suppressing the Doppler broadening as well. The reason for the increase in the dephasing rate at higher driving

frequencies beyond 3 kHz appears to result from the excitation of other momentum modes along with wavepacket spreading in momentum space.

Thirdly, we note that we can use the measured decay rates of  $P_{tot}(t)$  and  $N_k/(N_0 + N_k)(t)$  to isolate and estimate the decay due to collisions. We thus measure the collisional cross section to be  $7.1(\pm 1.8) \times 10^{-16} m^2$  in agreement with the known [17] value of  $8.37 \times 10^{-16} m^2$  [19].

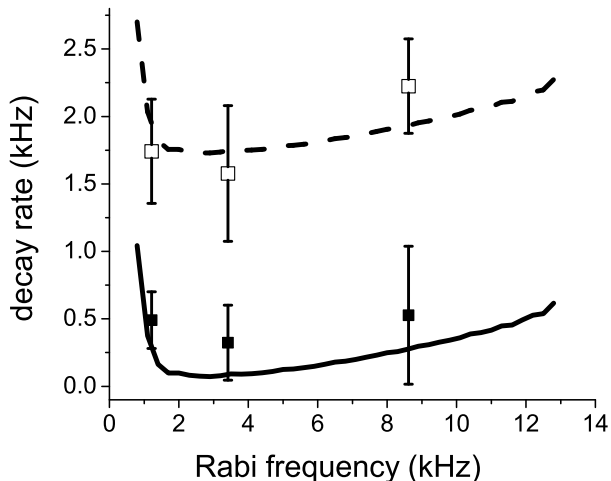


FIG. 5: Measured decay rates as a function of oscillation frequency. The solid boxes are the exponential fit decay rates of the oscillations in the post-selected  $N_k/(N_0 + N_k)$ . The solid line is the rate of decay fitted to the results of GPE simulations. The open boxes are the fitted decay rates of average momentum  $P_{tot}$ . The dashed line is the sum of the expected LDA collision rate (1.66 kHz) with the decay rates from GPE simulations (solid line).

In conclusion, we measure a suppression of the mean-field shift for a strong excitation of the BEC. We also observe an order of magnitude suppression of the inhomogeneous broadening and Doppler broadening mechanisms between strongly driven colliding Bose-Einstein condensates. Furthermore, we measure a collisional decoherence rate in agreement with that expected from previous measurements.

In the future we hope to observe a splitting in a Bragg probe spectrum from such a strongly driven system. We also hope to measure a shift in the energy of the excitations due to off-resonance Bragg pulses, in analogy with the ac Stark shift. This shift may even modify the collision rate by shifting the resonance energy sufficiently to influence the interaction with the finite width collisional quasi-continuum [20].

This work was supported in part by the Israel Ministry of Science, the Israel Science Foundation and by Minerva

foundation.

- 
- [1] F. Zambelli, L.P. Pitaevskii, D.M. Stamper-Kurn, and S. Stringari, Phys. Rev. A **61**, 063608 (2000).
  - [2] J. Stenger et al., Phys. Rev. Lett. **82**, 4569, (1999).
  - [3] N. Katz, J. Steinhauer, R. Ozeri, N. Davidson, Phys. Rev. Lett. **89**, 220401 (2002).
  - [4] C. Cohen-Tannoudji, J. Dupont-Roc and G. Grynberg, *Atom-Photon interactions*, John Wiley & Sons Inc. (1992).
  - [5] D.M. Stamper-Kurn et al., Phys. Rev. Lett. **83**, 2876 (1999).
  - [6] J. Steinhauer et al., Phys. Rev. Lett. **90**, 060404 (2003).
  - [7] A. Brunello, F. Dalfovo, L. Pitaevskii, S. Stringari, and F. Zambelli, Phys. Rev. A **64**, 063614 (2001).
  - [8] E. W. Hagley et al., Phys. Rev. Lett. **83**, 3112, (1999). M. Trippenbach et al., J. Phys. B, **33**, 47 (2000).
  - [9] S. Richard et al., Phys. Rev. Lett. **91**, 010405 (2003); D. Hellweg et al., Phys. Rev. Lett. **91**, 010406 (2003).
  - [10] For concreteness we denote the dephasing time by the  $1/e$  decay time of the cosine transform of the lineshape. The dephasing rate is the inverse of the dephasing time. This corresponds to an analytical estimate of the decay rate of the Ramsey fringes.
  - [11] We numerically solve the GPE for the order parameter of the condensate  $i\hbar\partial_t\psi = \{-\hbar^2\nabla^2/2m + V + g|\psi|^2\}\psi$ , with the time dependant external potential typically of the form  $V(\mathbf{r}, t) = m/2(\omega_r^2 r^2 + \omega_z^2 z^2) + \Omega(t)V_B \cos(kz - \delta\omega t)$ .  $V_B$  is the two-photon Rabi Bragg frequency, and  $\Omega(t)$  is a general envelope function. All other parameters for the simulation are as in the experimental system, described above. The ground-state is found for  $t < 0$  by imaginary time evolution. We exploit the cylindrical symmetry to evolve the wavefunction on a two dimensional grid  $N_z \times N_r$  ( $4096 \times 32$ ), using the Crank-Nicholson differencing method along with the alternating direction implicit algorithm.
  - [12] M. G. Moore and P. Meystre, Phys. Rev. Lett. **83**, 5202 (1999).
  - [13] C. Cohen-Tannoudji and C. Robilliard, C. R. Acad. Sci. Paris, t. 2, Srie IV, 445, (2001).
  - [14] J. Steinhauer, R. Ozeri, N. Katz and N. Davidson, Phys. Rev. Lett. **88**, 120407 (2002).
  - [15] T. Esslinger, I. Bloch, and T. W. Hänsch, Phys. Rev. A **58**, R2664 (1998).
  - [16] M. Kozuma et al., Phys. Rev. Lett. **82**, 871 (1999).
  - [17] H.M.J.M. Boesten, C.C. Tsai, J.R. Gardner, D.J. Heinzen, and B.J. Verhaar, Phys. Rev. A **55**, 636 (1997).
  - [18] M. Krämer, C. Menotti, L. Pitaevskii, S. Stringari, cond-mat/0305300.
  - [19] For weak excitations, at our experimental parameters, we expect a significant suppression of the collisional cross section as compared to the free particle value [3] ( $\sim 35\%$ ). However, for strong excitations we do not expect such a large suppression, since the perturbative assumptions do not apply.
  - [20] A. G. Kofman and G. Kurizki, Phys. Rev. Lett. **87**, 270405 (2001).